

Generalized unitarity at work: first NLO QCD results for hadronic $W + 3$ jet production

R. Keith Ellis

Fermilab, Batavia, IL 60510, USA
Email: ellis@fnal.gov

Kirill Melnikov

Department of Physics and Astronomy, Johns Hopkins University, Baltimore, MD 21218, USA
Email: melnikov@pha.jhu.edu

Giulia Zanderighi

Rudolf Peierls Centre for Theoretical Physics, 1 Keble Road, University of Oxford, UK
Email: g.zanderighi1@physics.ox.ac.uk

ABSTRACT: We compute the leading color, next-to-leading order QCD corrections to the dominant partonic channels for the production of a W boson in association with three jets at the Tevatron and the LHC. This is the first application of generalized unitarity for realistic one-loop calculations. The method performs well in this non-trivial test and offers great promise for the future.

Contents

1. Introduction	1
2. Tree-level processes and subtraction terms	4
3. Integration over the phase-space	9
4. Virtual corrections	11
5. Results	12
6. Conclusions	16

1. Introduction

There are many multi-particle processes, knowledge of which through next-to-leading order (NLO) in QCD would be very desirable [1]. This statement, often repeated in the context of the forthcoming experiments at the LHC is, in fact, true even at the Tevatron. For example, the production rates for $W(Z) + n$ jets, with $n \leq 4$ are well measured [2, 3] at the Tevatron¹ but next-to-leading order QCD computations for such processes exist only for $n \leq 2$ [4].

Of course, there are good reasons for that. The NLO QCD computations for processes with a large number of external particles are difficult, both analytically and numerically; a list of well-known problems can be found in [1]. The need to overcome these difficulties has made the computation of one-loop multi-leg scattering amplitudes the focus of much research. In recent years, three main suggestions for possible solutions have emerged as a result.

First, it was argued, and demonstrated by explicit computations, that traditional methods, where one starts from Feynman diagrams and proceeds through a Passarino-Veltman [5] style reduction, can be optimized and made highly efficient [6–16]. Second, it was also shown that pure numerical approaches to NLO computations are feasible [17–23].

The third idea is the use of generalized unitarity where one starts from on-shell tree-level scattering amplitudes and recycles them into loops. The idea of generalized unitarity was proposed in Ref. [24] more than ten years ago. Important physical results obtained using this method [25] have demonstrated both its potential and limitations. The techniques of applying generalized unitarity were significantly developed in recent years thanks

¹Currently, for total cross-sections, errors range from ten percent for $W + 1$ jet to fifty percent for $W + 4$ jets. The error on $W + 3$ jets production cross-section is about twenty percent [2, 3].

	W^\pm , TeV	W^+ , LHC	W^- , LHC
σ [pb], $\mu = 40$ GeV	74.0 ± 0.2	783.1 ± 2.7	481.6 ± 1.4
σ [pb], $\mu = 80$ GeV	45.5 ± 0.1	515.1 ± 1.1	316.7 ± 0.7
σ [pb], $\mu = 160$ GeV	29.5 ± 0.1	353.5 ± 0.8	217.5 ± 0.5

Table 1: The leading order total cross section for the production of a W boson in association with three jets including both two quark and four quark processes vs. factorization and normalization scale. The results are obtained using the program MCFM. Cuts for the jets are $p_T > 15$ GeV, $|\eta| < 2$ at the Tevatron ($\sqrt{s} = 1.96$ TeV) and $p_T > 50$ GeV, $|\eta| < 3$ at the LHC ($\sqrt{s} = 14$ TeV). The CTEQ6L1 parton distributions which have $\alpha_s(M_Z) = 0.13$ are used. The quoted errors are statistical only.

to important advances in Refs. [26–30]. These developments led to the design of two generalized unitarity algorithms [31, 32]. These methods are seminumerical in the sense that they depend on the complete analytic knowledge of the relevant scalar integrals [33].

The computational algorithm suggested in Ref. [32] is employed in this paper; we will refer to it as D -dimensional generalized unitarity. Note that this method was recently used to obtain results not currently attainable with other methods, see e.g. Refs. [34–36]. However, an apparent weakness of generalized unitarity is that no result for a physical process has been obtained within this framework.² This should be contrasted with the traditional tensor reduction approaches which never lost contact with phenomenology and are being constantly refined to accommodate new challenges.

This is not a good situation for generalized unitarity which has to live up to the claim of its advocates that it is a more powerful method. The only way to address this potential criticism is to demonstrate the applicability of generalized unitarity in actual calculations of direct phenomenological interest, preferably in processes which are beyond the reach of traditional methods. We have chosen the production of a W boson in association with three jets for this purpose. The reasons for our choice are as follows:

- the calculation of NLO QCD corrections to this process is of direct relevance since it is measured at the Tevatron [2, 3]; it is not possible to use the leading order (LO) prediction for a serious comparison of theoretical and experimental results because the LO cross section varies by as much as a factor of two under reasonable changes in renormalization and factorization scales, see e.g. Table 1;
- measurements at the Tevatron have shown that for $W + n$ jets with $n = 1$ and 2, the data [2, 3] is well described by NLO QCD [4]; it is interesting to verify this also for three and higher numbers of jets;
- $W + 3$ jet production is of interest for the LHC, being one of the backgrounds to model-independent searches for new physics using the jets plus missing energy signal;

²We distinguish between generalized unitarity and application of the algorithm of Ref. [28] to Feynman diagrams. The latter method was employed for the computation of NLO QCD corrections to a relatively simple physical process $pp \rightarrow VVV$ in [37].

	$W, \sqrt{s} = 1.96 \text{ TeV},$	$W^+, \sqrt{s} = 14 \text{ TeV},$	$W^-, \sqrt{s} = 14 \text{ TeV},$
$\sigma_{2q}^{\text{full}} [\text{pb}]$	29.63 ± 0.04	356.99 ± 0.77	216.35 ± 0.40
$\sigma_{2q}^{\text{lc}} [\text{pb}]$	32.96 ± 0.02	377.08 ± 0.79	229.89 ± 0.42
$\sigma_{4q}^{\text{full}} [\text{pb}]$	16.13 ± 0.03	147.60 ± 0.38	94.91 ± 0.19
$\sigma_{4q}^{\text{lc}} [\text{pb}]$	16.12 ± 0.02	153.36 ± 0.36	97.64 ± 0.22

Table 2: Full and leading color cross sections for the production of a W boson and three jets for the two- (2q) and four-quark (4q) processes, at leading order. Cuts, parton distributions and scale choices as in Tab. 1. The renormalization and factorization scale is set equal to 80 GeV.

- the calculation of NLO QCD corrections to $W + 3$ jet production is highly non-trivial: there are 1583 Feynman diagrams including a significant number of high-rank six-point functions. There is no doubt that the computation of NLO QCD corrections to this processes is a challenging task for traditional diagrammatic approaches.

In our opinion these reasons make $W + 3$ jet production an ideal testing ground for the unitarity method and, recently, we made the first step in that direction. In Ref. [36] the three current authors, together with Giele and Kunszt, applied the generalized D -dimensional unitarity method to compute all one-loop matrix elements needed for the NLO corrections to $W + 3$ jet production including two-quark ($q\bar{q}gggW$) and four-quark ($q\bar{q}Q\bar{Q}W$) partonic processes [36]. Leading color two-quark amplitudes were also computed in Ref. [38].

With the virtual corrections in hand, two more steps are required to arrive at physical predictions for $W + 3$ jet production. First, the virtual corrections should be integrated over the relevant phase-space. Second, we need to consider processes with one additional parton in the final state. When this parton becomes soft or collinear to other partons in the process, the final state that consists of four partons contributes to the final state with three hard jets.

In spite of all the technical improvements described above, the computation of the matrix elements for $W + 5$ partons at one-loop and $W + 6$ partons at tree-level and integrating them over the phase-space are very challenging tasks. For this reason it is useful to look for approximations, which help to reduce the technical complexity of the problem and are justifiable from a physics viewpoint. An obvious possibility is to consider the large- N_c approximation.

To check how well this approximation works, we study leading order results for $W + 3$ jet production. A compilation of results using the program MCFM [4] is given in Tables 2,3. It follows from these Tables that, both at the Tevatron and the LHC, two-quark processes dominate over four-quark processes.³ At both colliders two-quark processes provide about 70% of the observed cross-section, with four-quark processes being responsible for the remaining 30%. Also, the large- N_c approximation turns out to be good to about 10% for both the Tevatron and the LHC. We therefore conclude that a useful first step towards

³We show numbers for fixed renormalization and factorization scales, but the relative decomposition into channels is largely scale-independent.

	$W, \sqrt{s} = 1.96 \text{ TeV}, p\bar{p}$	$W^+, \sqrt{s} = 14 \text{ TeV}, pp$	$W^-, \sqrt{s} = 14 \text{ TeV}, pp$
σ [pb]	32.96 ± 0.02	377.08 ± 0.79	229.89 ± 0.42
gg [%]	2.60	6.80	11.16
qg [%]	49.76	37.90	34.51
gq [%]	2.35	37.86	34.42
$g\bar{q}$ [%]	19.89	7.97	9.33
$\bar{q}g$ [%]	3.63	7.99	9.38
$\bar{q}\bar{q}$ [%]	0.0	0.0	0.0
qq [%]	0.0	0.0	0.0
$q\bar{q}$ [%]	21.52	0.73	0.60
$\bar{q}q$ [%]	0.26	0.73	0.60

Table 3: The cross section for the production of a W and three jets at leading color for the two quark processes and the percentages contributed by various incoming channels. Cuts and parton distributions as in Table 1. The renormalization and factorization scale is set equal to 80 GeV.

computing NLO QCD corrections to $W + 3$ jet production cross-section is the calculation of those corrections for partonic processes with *only* two quarks in the initial and/or final state, in the large- N_c approximation. Because the contribution of gg channel is small both at the Tevatron and the LHC, we may further limit ourselves to study processes with at least a quark or an anti-quark in the initial state, namely the six incoming channels $q\bar{q}, \bar{q}q, qg, \bar{q}g, gq$, and $g\bar{q}$. As we explain below, by working in the large- N_c approximation and by considering the two-quark channels only, we can simplify the calculation significantly.

The remainder of the paper is organized as follows. In Section 2 the computation of real emission corrections is described; the integration of the $W + 6$ parton matrix elements squared over the available phase-space is discussed in Section 3. In Section 4 the calculation of the virtual corrections performed in Ref. [36] is reviewed. In Section 5 numerical results are presented. We conclude in Section 6.

2. Tree-level processes and subtraction terms

In this Section we discuss the computation of the relevant tree-level scattering amplitudes. We need these amplitudes to calculate the production cross-section for $W + 3$ jets at tree level as well as the real emission correction to that process from the $W + 4$ parton final state. In what follows, we present matrix elements that describe the production of a W^+ boson, but everything that we say can be adapted to the case of W^- production, after obvious modifications.

The scattering amplitude for the process $0 \rightarrow \bar{u} + d + n g + W^+$ can be decomposed into color-ordered amplitudes according to the equation

$$\mathcal{A}_n^{\text{tree}}(1_{\bar{u}}, 2_d, 3_g, \dots, n_g) = g^{n-2} \sum_{\sigma \in S_{n-2}} (T^{a_{\sigma(3)}} \dots T^{a_{\sigma(n)}})_{i_2}^{\bar{i}_1} A_n(1_{\bar{u}}, 2_d; \sigma(3)_g, \dots, \sigma(n)_g). \quad (2.1)$$

In Eq. (2.1) g is the strong coupling constant and S_{n-2} denotes the $(n-2)!$ permutations of the gluons. Note that neither the W boson nor the electroweak couplings and CKM matrix elements are displayed in Eq. (2.1). We employ a normalization of the color $SU(3)$ generators such that $\text{Tr}(T^a T^b) = \delta^{ab}$.

To calculate the production cross-section, we need to square the matrix element in Eq. (2.1) and sum over the color and spin degrees of freedom of the quarks and gluons. In the large- N_c limit, individual color-ordered amplitudes do not interfere and we obtain the scattering amplitude squared

$$\sum_{\text{col, hel}} |\mathcal{A}_n^{\text{tree}}(1_{\bar{u}}, 2_d, 3, \dots, n)|^2 = (g^2)^{n-2} X_n \sum_{\text{hel}, S_{n-2}} |A_n(1_{\bar{u}}, 2_d; \sigma(3), \dots, \sigma(n))|^2, \quad (2.2)$$

where $X_n = (N_c^2 - 1)N_c^{n-3}$. Note that we decided to keep some terms in the factor X_n which are subleading in the large- N_c limit.

To arrive at the production cross-section, we need to choose a partonic initial state, square the scattering amplitude and integrate it over the phase-space available for the final state particles. Each choice of the initial state ij leads to a particular number of identical particles in the final state that we denote by N_{ij} . When the integration over the phase-space available for final state particles is performed, we have to divide the result by the symmetry factor $S_{ij} = N_{ij}!$. If we combine the symmetry properties of the phase-space with the fact that no interference terms are present in Eq. (2.2), we can reduce the number of scattering amplitudes that need to be calculated.

For example, if the initial state is $u\bar{d}$, extreme simplifications occur. In this case the final state is $W + (n-2)g$, and the number of identical gluons is $N_{u\bar{d}} = n-2$, leading to a symmetry factor $S_{u\bar{d}} = N_{u\bar{d}}! = (n-2)! = S_{n-2}$. We therefore write

$$\begin{aligned} \sigma_{u\bar{d}} &\sim \int \frac{d\phi_{\text{glue}}}{S_{u\bar{d}}} \sum_{\text{col, hel}} |\mathcal{A}_n^{\text{tree}}|^2 = (g^2)^{n-2} \frac{X_n}{S_{u\bar{d}}} \int d\phi_{\text{glue}} \sum_{\text{hel}, S_{n-2}} |A_n(1_{\bar{u}}, 2_d; \sigma(3), \dots, \sigma(n))|^2 \\ &= (g^2)^{n-2} X_n \int d\phi_{\text{glue}} \sum_{\text{hel}} |A_n(1_{\bar{u}}, 2_d; 3_{g_3}, 4_{g_4}, \dots, n_{g_n})|^2, \end{aligned} \quad (2.3)$$

where in the last step we used the symmetry of the $(n-2)$ -gluon phase-space, $d\phi_{\text{glue}}$, to argue that all color-ordered amplitudes give identical contributions to the cross-section. Since Eq. (2.3) is the consequence of the fact that gluons are identical particles, it holds true independently of cuts or other restrictions imposed on partons in the final state.

Other partonic channels can be simplified in a similar manner although, typically, we gain less compared to the $u\bar{d}$ initial state. For example, if we consider the initial state composed of a quark or anti-quark and a gluon, there are $(n-3)$ identical gluons in the final state. Therefore, the symmetry factor is $S_{qg} = (n-3)!$ and the number of independent color-ordered amplitudes that need to be considered is $S_{(n-2)}/S_{qg} = (n-2)$. For 3-parton final states $n=5$, so that there are three independent amplitudes while for 4-parton final states, $n=6$ and the number of independent amplitudes is four. When these numbers are compared to the $S_3 = 6$ and $S_4 = 24$ independent amplitudes that would be required if fixed ordering of the final state particles were discarded, we see that the improvement is substantial.

When the matrix element with $W + 4$ partons in the final state is integrated over the phase-space subject to the requirement that three jets are observed, divergent results are obtained. These divergences arise from phase-space regions where one of the four partons in the final state becomes soft or two partons become collinear to each other; eventually, they cancel against similar divergences in the virtual corrections. To achieve this cancellation in practice, divergences in real emission contributions need to be extracted. To make those divergences manifest, we use a subtraction method [39] as formulated by Catani and Seymour [40] who proposed simple subtraction terms, which they called dipoles. However, we need to make minor modifications to the Catani-Seymour formalism because we work with amplitudes where the ordering of identical particles in the final state is fixed.

To find dipole subtraction terms consistent with fixed ordering of the identical particles, it is convenient to follow the derivation in Ref. [40]. To this end, we calculate the soft limit of the amplitude squared, partial fraction the eikonal factors to isolate individual collinear limits, and extend the eikonal factors beyond the soft limits, taking Ref. [40] as an example. The dipoles that do not have soft singularities can be found by examining collinear limits of the contributing amplitudes. Although identical steps are required to find conventional dipoles, the difference between dipole terms that employ ordered and full amplitudes can be traced back to different soft limits and in the related necessity to go beyond the soft limit in a different way.

We now illustrate the construction of the subtraction terms by considering the $u\bar{d}$ initial state. Upon ordering the gluons in the final state, the cross-section is determined by the square of a single color-ordered amplitude summed over helicities. In the actual computation of the cross-section, this amplitude squared is multiplied by the infrared-safe measurement function F_J that depends on the momenta of n partons. We therefore define

$$\mathcal{D}(2; 3, 4 \dots n; 1) = \sum_{\text{hel}} |A_n(1_{\bar{u}}, 2_d, 3, \dots, n)|^2 F_J(1, 2, 3, \dots n), \quad (2.4)$$

where labels 1 and 2 denote incoming particles. Any gluon in the final state can become soft. We calculate the soft limit of the amplitude squared and obtain

$$\begin{aligned} \lim_{\text{soft}} \mathcal{D}(2; 3, 4, 5, 6; 1) &= s(5, 6, 1) \mathcal{D}(2; 3, 4, 5; 1) + s(4, 5, 6) \mathcal{D}(2; 3, 4, 6; 1) \\ &+ s(3, 4, 5) \mathcal{D}(2; 3, 5, 6; 1) + s(2, 3, 4) \mathcal{D}(2; 4, 5, 6; 1). \end{aligned} \quad (2.5)$$

The eikonal factor in Eq. (2.5)

$$s(i, j, k) = \frac{p_i p_k}{(p_i p_j)(p_j p_k)} \quad (2.6)$$

corresponds to the limit where momentum p_j is soft.⁴ Performing partial fractioning and extending eikonal factors beyond the soft limit, we obtain the expression for the subtraction term

$$\mathcal{D}_{\text{sub}}(2; 3, 4, 5, 6; 1) = \tilde{D}_{61,5}^{gg} \otimes \mathcal{D}(2; 3, 4, \tilde{5}; \tilde{1}6) + \tilde{D}_{65,1}^{gg} \otimes \mathcal{D}(2; 3, 4, \tilde{5}6; \tilde{1})$$

⁴We use a convention of treating all particles as if in the final state and as if all the momenta are outgoing. This allows us to write the soft limit in Eq. (2.5) in a symmetric way.

$$\begin{aligned}
& +\tilde{D}_{54,6}^{gg} \otimes \mathcal{D}(2; 3, \tilde{4}\tilde{5}, \tilde{6}; 1) + \tilde{D}_{56,4}^{gg} \otimes \mathcal{D}(2; 3, \tilde{4}, \tilde{5}\tilde{6}; 1) + \tilde{D}_{43,5}^{gg} \otimes \mathcal{D}(2; \tilde{3}\tilde{4}, \tilde{5}, 6; 1) \\
& +\tilde{D}_{45,3}^{gg} \otimes \mathcal{D}(2; \tilde{3}, \tilde{4}\tilde{5}, 6; 1) + \tilde{D}_{34,2}^{gg} \otimes \mathcal{D}(\tilde{2}; \tilde{3}\tilde{4}, 5, 6; 1) + \tilde{D}_{32,4}^{gg} \otimes \mathcal{D}(\tilde{2}\tilde{3}; \tilde{4}, 5, 6; 1). \quad (2.7)
\end{aligned}$$

The notation $\tilde{i}\tilde{j}$ and \tilde{j} in Eq. (2.7) are the standard notations, see Ref. [40]. The mapping between momenta $p \rightarrow \tilde{p}$ that is required to evaluate the right hand side in Eq. (2.7) is constructed in the same way as in Ref. [40]. The dipole functions $\tilde{D}_{ij,k}^{\text{fl}_i, \text{fl}_j}$ that we introduced in Eq. (2.7) are closely related to the original Catani-Seymour dipoles [40] and we explain the exact correspondence below. Before going into this, we point out that a modification of the subtraction terms is required to remove the symmetry between the emitter and emitted partons, inherent in final-final and final-initial dipoles in the original formulation by Catani and Seymour.⁵ In our notation, the non-integrable singular limit of the dipole $\tilde{D}_{ij,k}$ is associated with the soft limit of parton i whereas the soft limit of parton j does not introduce a non-integrable singularity.

To make things clear, we give examples of dipoles that we employ in the present calculation. For final-final dipoles, where both emitter and emitted partons are gluons, we use

$$\begin{aligned}
\tilde{D}_{ij,k}^{gg} \otimes \mathcal{D}(2; ..\tilde{i}\tilde{j}, \tilde{k}..; 1) &= \frac{1}{(p_i p_j)} \left[-g_{\mu\nu} \left(\frac{1}{1 - z_j(1 - y_{ij,k})} - 1 \right) \right. \\
& \left. + (1 - \epsilon) \frac{l_\mu l_\nu}{2p_i p_j} \right] A_5(2; ..\tilde{i}\tilde{j}_\mu, \tilde{k}..; 1) A_5^*(2; ..\tilde{i}\tilde{j}_\nu, \tilde{k}..; 1), \quad (2.8)
\end{aligned}$$

where $\epsilon = (4 - D)/2$ is the parameter of dimensional regularization, and $y_{ij,k} = p_i p_j / (p_i p_j + p_i p_k + p_j p_k)$, $z_j = p_j p_k / (p_i p_k + p_j p_k)$ and $l = (1 - z_j)p_i - z_j p_j$. The momenta of particles $\tilde{i}\tilde{j}$ and \tilde{k} are [40]

$$p_{\tilde{i}\tilde{j}} = p_i + p_j - \frac{y_{ij,k}}{1 - y_{ij,k}} p_k, \quad p_{\tilde{k}} = \frac{p_k}{1 - y_{ij,k}}. \quad (2.9)$$

In Eq. (2.8) $A(..i\tilde{j}_\mu...)$ denotes the tree level amplitude with the polarization vector for particle $i\tilde{j}$ removed.

For final-initial dipoles, where both emitter and emitted partons are gluons, we use

$$\begin{aligned}
\tilde{D}_{ij,a}^{gg} \otimes \mathcal{D}(..\tilde{i}\tilde{j}, ..\tilde{a}) &= \frac{1}{p_i p_j x_{ij,a}} \left[-g_{\mu\nu} \left(\frac{1}{1 - z_j + (1 - x_{ij,a})} - 1 \right) \right. \\
& \left. + (1 - \epsilon) \frac{l_\mu l_\nu}{2p_i p_j} \right] A_5(..\tilde{i}\tilde{j}_\mu, ..\tilde{a}) A_5^*(..\tilde{i}\tilde{j}_\nu, ..\tilde{a}), \quad (2.10)
\end{aligned}$$

where $x_{ij,a} = 1 + p_i p_j / (p_i p_a + p_j p_a)$ and $z_j = p_j p_a / (p_i p_a + p_j p_a)$ and $l = (1 - z_j)p_i - z_j p_j$. Note that the plus-sign between the first and the second term in the equation for $x_{ij,a}$ is the consequence of the all-outgoing momentum convention.

For initial-final dipoles, where emitter and emitted parton are quark and gluon respectively, we use

$$\tilde{D}_{ia,k}^{gq} \otimes \mathcal{D}(\tilde{k}..\tilde{i}\tilde{a}) = \frac{1}{2(p_i p_a) x_{ia,k}} \left[\frac{2}{1 - x_{ia,k} + u_i} - (1 + \epsilon) - x_{ia,k}(1 - \epsilon) \right] |A_5(\tilde{k}..\tilde{i}\tilde{a})|^2, \quad (2.11)$$

⁵For initial-final and initial-initial dipoles this symmetry is not present to begin with and we use standard expressions for those dipoles.

where $x_{ia,k} = 1 + p_i p_k / (p_i p_a + p_k p_a)$, $u_i = p_i p_a / (p_i p_a + p_k p_a)$.

The subtraction terms for all other partonic channels are constructed along similar lines. Since more orderings contribute to the amplitude squared for partonic channels other than $u\bar{d}$ and $\bar{d}u$, more dipoles need to be considered to account for all the singular limits. Initial-initial dipoles appear for all channels except $u\bar{d}$ and $\bar{d}u$. Finally, let us note that the need to subtract certain dipoles cannot be established from the soft limit of the amplitude. In those case, the analysis of collinear singularities of the amplitude squared is required to determine the dipoles that need to be subtracted.

We also note that a simple but extremely useful modification of the Catani-Seymour dipoles was suggested by Nagy [41]. The idea is to limit the subtraction to a small region of phase-space available for final-state particles. To this end, final-final dipoles are multiplied by $\theta(\alpha - y)$, final-initial dipoles by $\theta(\alpha - (1 - x))$, initial-final dipoles by $\theta(\alpha - u)$ and initial-initial dipoles by $\theta(\alpha - v)$ where y, x, u and v are standard variables used in [40]. This has the advantage that the subtraction is not performed if the kinematics of four-parton final state is far away from the singular limit, leading to a considerable saving in computing time, because the matrix element squared associated with the excluded dipole need not be computed.

As we have seen, the construction of the dipoles relevant for our purposes is straightforward and requires only small modifications compared to the original formalism of Catani and Seymour. The next step in the subtraction program – the integration of the subtracted terms over the unresolved phase-space – is even more straightforward since the integrals of our modified dipoles can be easily extracted from the results quoted in Ref. [40]. To see this, note that for initial-final and initial-initial dipoles, we do not introduce any modifications relative to Ref. [40]. We do modify final-final and final-initial dipoles, but there is a simple relationship between our dipoles \tilde{D} and the ones in Ref. [40], D_{CS} . For example, for final-final dipole, we can write

$$D_{\text{CS}}(z, y) = \tilde{D}(z, y) + \tilde{D}(1 - z, y). \quad (2.12)$$

To compute the integral of the subtraction term, we need to integrate $\tilde{D}(z, y)$ over y and z

$$\int_0^1 dy \, dz f(z, y) \tilde{D}(z, y), \quad (2.13)$$

where $f(z, y)$ is the weight function. The important property of the weight function is that it is symmetric with respect to $z \rightarrow 1 - z$ transformation. Because of this symmetry property, we conclude that

$$2 \int_0^1 dy \, dz f(z, y) \tilde{D}(z, y) = \int_0^1 dy \, dz f(z, y) D_{\text{CS}}(z, y). \quad (2.14)$$

Since the integral that appears on the right hand side of that equation is computed in [40], $\int \tilde{D}(z, y)$ can be easily extracted. A similar reasoning can be used to obtain integrals of the final-initial dipoles.

3. Integration over the phase-space

The next issue to be discussed is the integration of the difference between the matrix element squared and the subtraction term over the entire phase-space allowed by the external cuts. We use VEGAS [42] to adapt the integration grid automatically but we still need to generate the parton kinematics carefully to ensure efficient sampling.

In addition, when trying to integrate over the phase-space, we face a difficulty inherent in any subtraction method. To illustrate the issue, consider a matrix element squared that requires a subtraction of a particular final-final dipole to make it integrable. The dipole is described by two standard variables y and z . The matrix element squared has non-integrable singularities at $y = 0$, $z = 0$ and at $y = 0$, $z = 1$; these singularities are removed by subtraction. The difference between the matrix element and the subtraction term is still singular, but these singularities are integrable. We assume that the difference scales as $1/\sqrt{y}$ and as $1/\sqrt{z}$ or $1/\sqrt{1-z}$. Although these are integrable singularities, in order to have the standard estimate of the integration error when using Monte-Carlo integration techniques, it is mandatory to change integration variables to absorb the square-root singularities into the measure.

Since we have a left-over square-root singularity for every dipole that we need to subtract from the matrix element squared, we need to do a large number of variable transformations if we want to absorb all the singularities. Note also that different dipoles need to be subtracted for different initial states. This means that the required changes of variables can not be done globally and, instead, we have to adopt a multichannel integration technique. To this end, for each partonic channel, we

- randomly pick a dipole that contributes to a chosen channel – all dipoles are given equal weights;
- generate the phase-space for the chosen dipole in such a way that the square-root singularity can be absorbed into the integration measure.

More specifically, suppose we are interested in the contribution of a particular partonic channel to the production cross-section for which N_d dipoles are required to make it finite. We need to compute

$$I = \int d\phi_4 (|A|^2 - |A|_{\text{subtr}}^2), \quad (3.1)$$

where $d\phi_4$ denotes the phase-space with four partons in the final state, $|A|^2$ is the matrix element squared and $|A|_{\text{subtr}}^2$ is the subtraction term. We rewrite the integral as

$$I = \sum_{n=1}^{N_d} \alpha_n I_n, \quad (3.2)$$

where α_n are some constants and

$$I_n = \int \frac{d\phi_4}{J_n} \frac{(|A|^2 - |A|_{\text{subtr}}^2)}{\sum_m \alpha_m J_m^{-1}}. \quad (3.3)$$

In Eq. (3.3) J_n are Jacobian factors. In the actual calculation, we choose the coefficients α_n to be equal although, in principle, it is possible to optimize their choice iteratively.

We associate each I_n with a particular dipole contribution that needs to be subtracted from the matrix element squared. Suppose that n is a final-final dipole. We start by generating the phase-space for *three massless* partons and the W boson, assuming that the kinematics of the massless parton is characterized by a dp_\perp/p_\perp distribution (for transverse momentum p_T above the jet p_T cut) and by a uniform distribution in rapidity.⁶ Then, we use the fact that the four-parton phase-space factorizes into the product of the three-parton phase-space and the dipole phase-space that is completely specified by three additional variables. We denote the momenta of the three-parton final state as \tilde{p} , and momenta of the four-parton final state as p . Additional variables needed to describe the kinematics of the $3 \rightarrow 4$ splitting are y, z and ϕ . We therefore write

$$d\phi_4(p) = d\phi_3(\tilde{p}_{ij}, \tilde{p}_k) dp_i(\tilde{p}_{ij}, p_k), \quad (3.4)$$

and

$$dp_i(\tilde{p}_{ij}, p_k) = \frac{\tilde{p}_{ij}\tilde{p}_k}{8\pi^2} \frac{d\phi}{2\pi} dz_i dy_{ij,k} (1 - y_{ij,k}). \quad (3.5)$$

Having generated the momenta of three-parton final state \tilde{p} , we use them to construct the momenta p according to the following formulae

$$\begin{aligned} p_i &= z_i \tilde{p}_{ij} + y_{ij,k} z_j \tilde{p}_k + k_\perp, \\ p_j &= z_j \tilde{p}_{ij} + y_{ij,k} z_i \tilde{p}_k - k_\perp, \\ p_k &= (1 - y_{ij,k}) \tilde{p}_k, \\ p_{m \neq i,j,k} &= \tilde{p}_m. \end{aligned} \quad (3.6)$$

The transverse momentum reads $k_\perp^\mu = |k_\perp| (\cos \phi v_1^\mu + \sin \phi v_2^\mu)$ and $|k_\perp| = \sqrt{yz(1-z)2\tilde{p}_{ij}\tilde{p}_k}$. The two auxiliary vectors $v_{1,2}$ are such that $v_{1,2}^2 = -1$, $v_1 v_2 = 0$, $v_{1,2} \tilde{p}_{ij} = 0$, $v_{1,2} \tilde{p}_k = 0$.

The choice of the Jacobian factor J_n allows us to absorb the square-root singularities; for final/final dipoles we use the form suggested in Ref. [43]:

$$J_n^{-1} = \frac{\sqrt{z_i} + \sqrt{z_j}}{\sqrt{y_{ij,k}} \sqrt{z_i z_j}}. \quad (3.7)$$

Note that this Jacobian can be written in terms of the four parton momenta p , since, as follows from Eq. (3.7), we can express z_i, z_j and $y_{ij,k}$ in terms of these momenta,

$$z_i = \frac{p_i p_k}{p_i p_k + p_j p_k}, \quad z_j = 1 - z_i, \quad y_{ij,k} = \frac{p_i p_j}{p_i p_k + p_j p_k + p_i p_j}. \quad (3.8)$$

This remark is important since, as follows from Eq. (3.3), each integral I_n requires the knowledge of all Jacobians J_m including the ones with $m \neq n$. This, however, is not a problem because all those Jacobians are *uniquely* expressed through momenta p in the spirit of Eqs. (3.7) and (3.8).

⁶This is the standard procedure in MCFM.

The Jacobian J_n can be absorbed into the measure by a simple change of variables

$$\frac{dp_i(\tilde{p}_{ij}, p_k)}{J_n} = \frac{\tilde{p}_{ij}\tilde{p}_k}{\pi^2} \frac{d\phi}{2\pi} d\mu_{ij,k} d\xi_i (1 - y_{ij,k}), \quad (3.9)$$

where

$$\bar{\phi} = \frac{\phi}{2\pi}, \quad y_{ij,k} = \mu_{ij,k}^2, \quad z_i = \frac{1}{2} \left(1 - (1 - 2\xi_i) \sqrt{1 + 4\xi_i(1 - \xi_i)} \right), \quad (3.10)$$

with $0 < \mu_{ij,k} < 1$ and $0 < \xi_i < 1$. So, given random numbers for μ, ξ , and $\bar{\phi}$ and the momenta of three-parton final state \tilde{p} , we can calculate z and y , the phase-space weight and the corresponding momenta p of the four-parton final state. We then calculate the matrix element squared as discussed in the previous Section and derive a particular contribution to the differential cross-section for $W + 3$ jet production.

Another case which requires comment involves dipoles where initial particles are present. We will consider the final-initial dipoles as an example. The general strategy is very similar to what has already been discussed. We start by generating momenta for the three-parton final state and the W -boson and three random numbers z, x and ϕ . We denote the momenta of one of the partons in the final state by \tilde{p}_{ij} and the momentum of the spectator in the initial state by \tilde{p}_a . We then generate the additional parton momentum according to the following formulae

$$\begin{aligned} p_i &= z\tilde{p}_{ij} + (1 - z)\frac{1 - x}{x}\tilde{p}_a + k_\perp, \\ p_j &= (1 - z)\tilde{p}_{ij} + z\frac{1 - x}{x}\tilde{p}_a - k_\perp, \\ p_a &= \frac{\tilde{p}_a}{x}, \end{aligned} \quad (3.11)$$

$$p_{m \neq i, a, k} = \tilde{p}_m, \quad (3.12)$$

where $k_\perp^\mu = |k_\perp| (\cos \phi v_1^\mu + \sin \phi v_2^\mu)$, $v_{1,2}^2 = -1$, $v_{1,2}\tilde{p}_{ij} = 0$, $v_{1,2}\tilde{p}_a = 0$ and $|k_\perp| = \sqrt{2\tilde{p}_{ij}p_a z(1 - z)(1 - x)}$.

For the final-initial dipole, we employ the Jacobian

$$J_n^{-1} = \frac{\sqrt{z} + \sqrt{1 - z}}{\sqrt{1 - x} \sqrt{z(1 - z)}}. \quad (3.13)$$

To absorb this Jacobian into the integration measure, we make a change of variables along the lines discussed in connection with final-final dipoles. Furthermore, we have to make sure that the new momenta of the initial parton p_a does not exceed the momentum of the proton since, a priori, the variable x can assume any value between 0 and 1. If the momentum of the initial state parton exceeds the momentum of the proton, the corresponding event is rejected. We deal with initial-final and initial-initial dipoles along similar lines.

4. Virtual corrections

A detailed description of the calculation of all one-loop amplitudes needed for the NLO correction to $W + 3$ jets at hadron colliders is given in Ref. [36]. Here we recall the elements of the discussion needed for the purpose of this paper.

At one-loop, using the color basis of Ref. [44] and neglecting contributions from closed fermion loops, the color decomposition for the process $0 \rightarrow \bar{u} + d + n \text{ } g + W^+$ can be written in terms of left primitive amplitudes [45] as

$$\mathcal{A}_n^{1\text{-loop}}(1_{\bar{u}}, 2_d, 3_g, \dots, n_g) = g^n \left[\sum_{p=2}^n \sum_{\sigma \in S_{n-2}} (T^{x_2} T^{a_{\sigma_3}} \dots T^{a_{\sigma_p}} T^{x_1})_{i_2}^{\bar{i}_1} (F^{a_{\sigma_{p+1}}} \dots F^{a_{\sigma_n}})_{x_1 x_2} \right. \\ \left. \times (-1)^n A_n^L(1_{\bar{u}}, \sigma(p)_g, \dots, \sigma(3)_g, 2_d, \sigma(n)_g, \dots, \sigma(p+1)_g) \right]. \quad (4.1)$$

In Eq. (4.1) for $p = 2$ the factor $(T \dots T)_{i_2}^{\bar{i}_1}$ becomes $(T^{x_2} T^{x_1})_{i_2}^{\bar{i}_1}$ and for $p = n$ the factor $(F \dots F)_{x_1 x_2}$ becomes $\delta_{x_1 x_2}$. As before neither the W boson nor the electroweak couplings and CKM matrix elements are displayed in Eq. (4.1). In the leading color approximation we retain only the $p = 2$ term and Eq. (4.1) simplifies to

$$\mathcal{A}_n^{1\text{-loop}}(1_{\bar{u}}, 2_d, 3_g, \dots, n_g) = g^n \left[\sum_{\sigma \in S_{n-2}} (T^{x_2} T^{x_1})_{i_2}^{\bar{i}_1} (F^{a_{\sigma_3}} \dots F^{a_{\sigma_n}})_{x_1 x_2} \right. \\ \left. \times (-1)^n A_n^L(1_{\bar{u}}, 2_d, \sigma(n)_g, \dots, \sigma(3)_g) \right]. \quad (4.2)$$

The matrix element squared is then given by

$$2 \sum_{\text{col, hel}} |\mathcal{A}_n^{1\text{-loop}}(1_{\bar{u}}, 2_d, 3_g, \dots, n_g) \mathcal{A}_n^{\text{tree},*}(1_{\bar{u}}, 2_d, 3_g, \dots, n_g)| \quad (4.3) \\ = 2 (N_c^2 - 1) N_c^{n-2} (g^2)^{n-1} \sum_{\text{hel}, S_{n-2}} |A_n^L(1_{\bar{u}}, 2_d, 3_g, \dots, n_g) A_n^*(1_{\bar{u}}, 2_d, 3_g, \dots, n_g)|,$$

where again we choose to keep some subleading color terms. We can now take advantage of the symmetry of the phase-space and fix the ordering of identical particles in the final state. The procedure is described in detail in Section 2.

5. Results

In this Section we present the results of our calculation of NLO QCD corrections to $W+3$ jet production. We begin by describing computational aspects of the problem. The total time needed for the calculation of virtual corrections is determined by how many one-loop primitive amplitudes must be evaluated and how computationally expensive they are. At leading color, we only need to calculate the fastest primitive amplitude, for which about 50 ms are required for a given momentum/helicity configuration.⁷

To compute the hadronic cross-section, we sum over six partonic channels. As explained in previous Sections, we fix the ordering of gluons in the final state. Then, for partonic channels with quark and anti-quark in the initial state, we evaluate the virtual primitive amplitudes $2^3 = 8$ times, since we sum over two helicities of each of the three gluons. For the $qg, gq, \bar{q}g, g\bar{q}$ channels we consider three different orderings of the final-state fermion, relative to the gluons. As the result, we evaluate $24 = 3 \times 2^3$ primitive

⁷All numbers are given for a computer with 2.33 GHz Pentium Xeon processor and Intel fortran compiler.

amplitudes per partonic channel with a single fermion in the initial state. Therefore, for the computation described in this paper, we need to compute the leading color primitive amplitude 112 times for each phase-space point. This translates into a total of 5.6 seconds per phase-space point.

This time is too large to allow us to compute the virtual corrections on a dynamical, self-adapting grid. We therefore adopt the following strategy for computing virtual corrections. First, we compute the tree level cross-section with a large number of points, 2×10^7 , and establish an integration grid.⁸ Once the grid is fixed, we compute virtual corrections by running three different jobs each with 10^5 evaluations using different seeds to start VEGAS off. We then average the results of these three evaluations. With this procedure, Monte Carlo errors for virtual corrections are around 0.7 – 1%.

For real corrections, we need about 10 msec per phase-space point to compute matrix element squared and the subtraction terms⁹. Since computation of the real emission correction is inexpensive, we calculate these corrections following the standard MCFM procedure of first doing a pre-conditioning run and then a final run. We used 10 times $4 \cdot 10^6$ points for the pre-conditioning run and five times $8 \cdot 10^6$ points for the final run. With this number of events, the Monte Carlo integration errors for the real (subtracted) contribution are around 0.4 – 0.7%.

As far as final results are concerned, errors coming from virtual and real corrections are comparable and the total Monte Carlo integration error is in the range of 1 – 4%; this is better than the theoretical uncertainty of the results estimated with a standard renormalization and factorization scale variation.

We are now in position to describe the numerical results of the computation. However, before we enter into this discussion, we remind the reader that our results are approximate for the following reasons:

- we employ the large- N_c approximation to compute the scattering amplitudes; using the leading order cross-section as a guide, we estimate that this approximation is accurate to about 10 percent;
- we include only the two-quark processes $q\bar{q}gggW$ and ignore the four-quark processes $q\bar{q}Q\bar{Q}gW$. Even within the two-quark processes, we do not consider the partonic channel with two gluons in the initial state. For the leading order cross-section, we find that the four-quark processes increase the cross-section by thirty percent so that omitting them gives results accurate to about thirty percent.

Because of these approximations, we warn the reader that absolute results for cross-sections and distributions that we report below should be used with caution. We believe,

⁸There are other ways to establish the grid. For instance, we can omit the computationally expensive parts of the virtual amplitudes and keep only logarithms of kinematic invariants that come from $1/\epsilon$ poles. We have checked that changing the strategy for establishing the grid has no bearing on the final result.

⁹This number depends on the value of the parameter α that determines how often subtraction terms need to be calculated [41]. The quoted value corresponds to $\alpha = 0.01$.

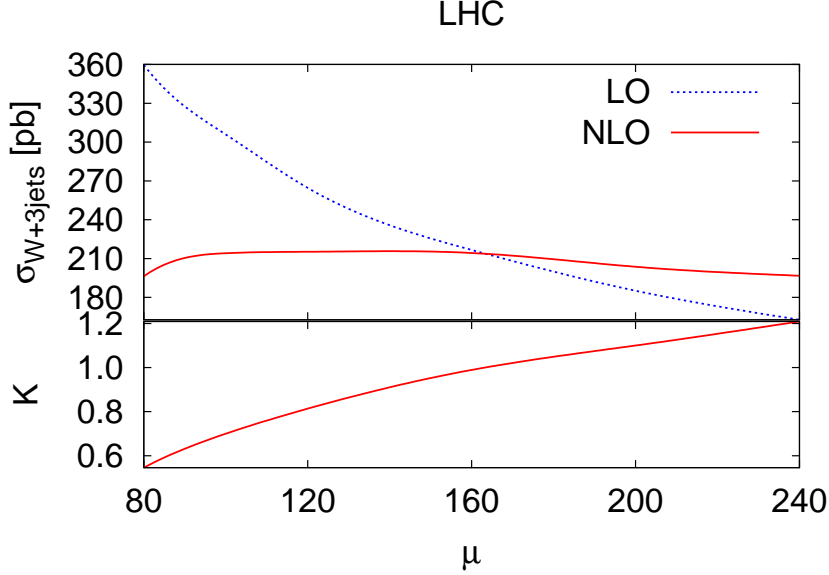


Figure 1: Inclusive $W^+ + 3$ jet cross-section at the LHC and the K -factor defined as $K = \sigma_{\text{NLO}}/\sigma_{\text{LO}}$ as a function of the renormalization and factorization scales. Jets are defined with k_T algorithm with $R = 0.7$ and $p_T > 50$ GeV. Jet rapidities satisfy $|\eta| < 3$. The LO and NLO cross-sections are computed with CTEQ6L1 and CTEQ6M parton distributions, respectively.

however, that ratios of NLO and LO results for various observables are less sensitive to these omissions.

The numerical results for $W + 3$ jet production at NLO are obtained using the CTEQ6m parton distributions [46] which have a value of $\alpha_S(M_z) = 0.118$. The evolution of the coupling constant is performed using the two-loop beta function

$$\beta(\alpha_s) = -b\alpha_s^2(1 + b'\alpha_s), \quad b = \frac{33 - 2n_f}{12\pi}, \quad b' = \frac{153 - 19n_f}{2\pi(33 - 2n_f)}, \quad (5.1)$$

where, in the spirit of the large- N_c approximation, we set the number of light flavors n_f equal to zero. The k_T jet algorithm with $R = \sqrt{\Delta\phi^2 + \Delta\eta^2} = 0.7$ and $p_T > 15$ GeV ($p_T > 50$ GeV) is used to define jet cross sections at the Tevatron and the LHC, respectively. We employ default MCFM choice for electroweak parameters and the CKM matrix elements; they can be found in Ref. [4].

In Figs. 1,2 we present total cross-sections and K -factors, defined as $K = \sigma_{\text{NLO}}/\sigma_{\text{LO}}$, for $W + 3$ jet production at the LHC and the Tevatron as a function of the factorization and the renormalization scales which we set equal to each other $\mu_R = \mu_F = \mu$. At the LHC, the NLO cross-section shows remarkable independence of the scale μ , unlike the LO result. The equality of LO and NLO cross-sections occurs at $\mu_0 \approx 160$ GeV. Because the dependence of the LO cross-section on the unphysical scale μ is strong, the NLO corrections are typically large. For example, choosing $\mu = m_W$ to compute the LO cross-section for $W + 3$ jet production at the LHC, leads to NLO QCD corrections of the order of -50% .

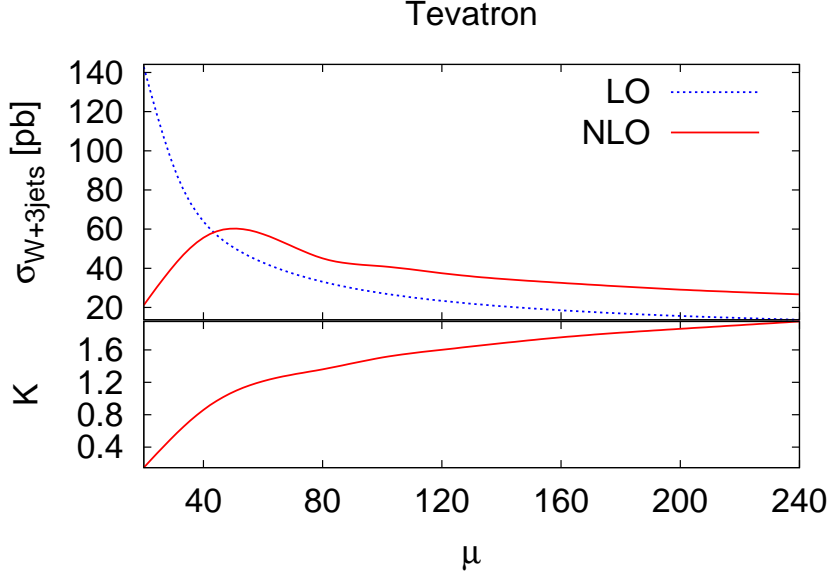


Figure 2: The inclusive $W + 3$ jet cross-section at the Tevatron and the K -factor defined as $K = \sigma_{\text{NLO}}/\sigma_{\text{LO}}$ as a function of the renormalization and factorization scales μ . Jets are defined with k_T algorithm with $R = 0.7$ and $p_T > 15$ GeV. Jet rapidities satisfy $|\eta| < 2$. The LO and NLO cross-sections are computed with CTEQ6L1 and CTEQ6M parton distributions, respectively.

For the Tevatron, the situation is different. First, the dependence of the NLO cross-section on the renormalization and factorization scales is sizeable although it is significantly reduced compared to the leading order cross-section. In addition, as follows from Fig. 2 the equality of leading and next-to-leading order cross-sections occurs at a scale $\mu_0 \approx 50$ GeV which is much smaller than the LHC case discussed above. This is not unexpected since both the center of mass energy and the p_\perp cut for jets is smaller at the Tevatron which leads to a much softer spectrum of jets compared to the LHC case.

It is interesting to note that gross features of NLO QCD corrections to $W + 3$ jet production, such as scales at which leading and next-to-leading order cross-sections coincide, are very similar to what was observed in NLO QCD computation of $W + 2$ jets [4, 47]. What differs between two and three jet production is the price one pays for making an infelicitous choice of scale in the LO result. Because the dependence on μ of $\sigma_{W+3 \text{ jet}}^{\text{LO}}$ is stronger than of $\sigma_{W+2 \text{ jet}}^{\text{LO}}$, K -factors for $W + 3$ jet decrease or increase stronger when one moves away from $\mu = \mu_0$.

Finally, we present selected results for differential distributions at the LHC. We choose the renormalization and factorization scales to be 160 GeV since this minimizes the inclusive K -factor. In Fig. 3 we plot the distribution in the variable H_T defined as the sum of transverse energies of jets, the missing transverse energy and the transverse energy of the lepton $H_T = \sum_j E_{\perp,j} + E_{\perp}^{\text{miss}} + E_{\perp}^e$. The variable H_T measures the overall hardness of a particular event and can be employed in model-independent searches for New Physics. As

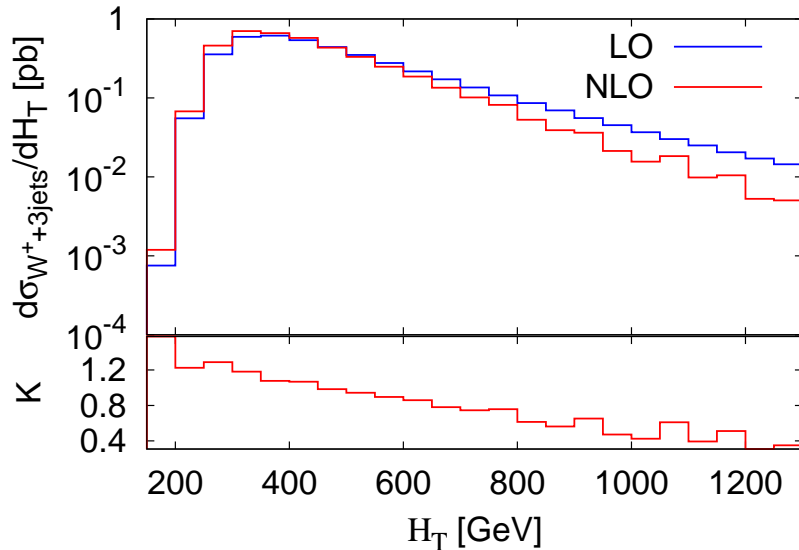


Figure 3: The distribution of the transverse energy $H_T = \sum_j E_{\perp,j} + E_{\perp}^{\text{miss}} + E_{\perp}^e$ and the K factor defined as $K = (d\sigma^{\text{NLO}}/dH_T) / (d\sigma^{\text{LO}}/dH_T)$ in $W^+ + 3$ jet inclusive production at the LHC at leading and next-to-leading order. Renormalization and factorization scales are set to 160 GeV.

illustrated Fig. 3, the H_T -distribution becomes softer at NLO, at least in comparison to the leading order result calculated at fixed scale $\mu = 160$ GeV.

In Fig. 4 we present the transverse momentum distribution of the third hardest jet in the inclusive production of $W + 3$ jets at the LHC. In the range of p_{\perp} shown in the plot, the shapes of p_{\perp} distributions at leading and next-to-leading order are nearly identical.

6. Conclusions

In this paper, we apply the method of generalized D -dimensional unitarity [32] to compute NLO QCD corrections to $W + 3$ jet production at the Tevatron and the LHC. There are two reasons that make this result an important benchmark in the field of one-loop QCD computations for hadron collider physics. First, this is the only application of the idea of generalized unitarity in a fully realistic one-loop computation that goes beyond calculation of one-loop helicity amplitudes at a fixed point in phase-space. Second, our result is one of the very few computations of one-loop corrections to six-parton processes at hadron colliders – the current research frontier in NLO QCD. It is remarkable that the method achieved this benchmark without a problem; this assures us that generalized unitarity is a practical computation method that can be applied to other, perhaps even more complicated, processes.

Looking into the near future, we expect to refine our computation in two ways. First, we expect to include the four-quark partonic channels in the large- N_c approximation; this is an important step for realistic phenomenology. Further down the road, we may want to

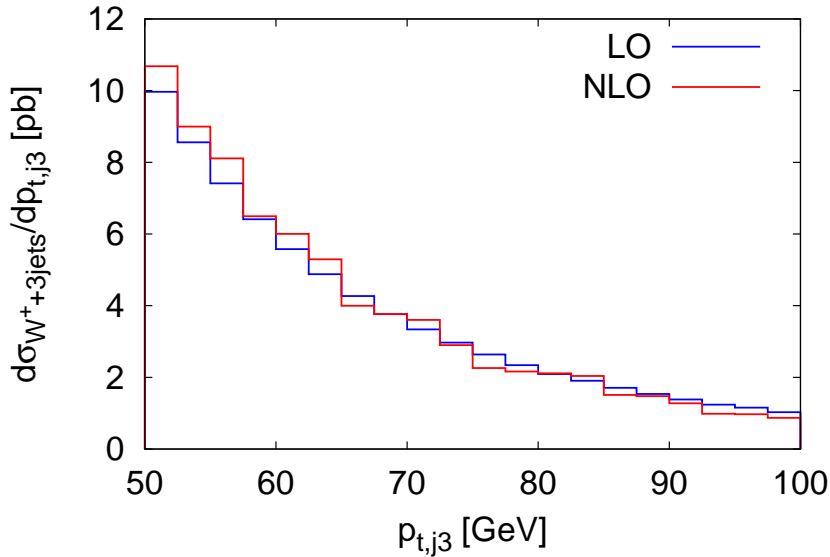


Figure 4: The transverse momentum distribution of the third hardest jet in the inclusive $W + 3$ jet production at the LHC. The renormalization and factorization scales are set to 160 GeV.

extend the computation beyond the leading color approximation. Estimating the increase in computer running time required to go beyond the large N_c limit, we find that about two minutes per point will be needed to compute virtual corrections to the matrix element squared. At face value, this is feasible, but computationally expensive. However, one can imagine various improvements, including Monte Carlo sampling over helicities and colors, that should lead to an appreciable improvement in the speed of the program.

Finally, we would like to say a few words about phenomenology. Since we did not consider the four-quark channels in this paper, we decided not to pursue very detailed phenomenological studies. However, the numerical results that we *do* report are instructive since they give an idea about potential significance of NLO QCD effects in $W + 3$ jet production at the Tevatron and the LHC. Our computation shows that NLO QCD effects are large and can reach $\pm 50\%$, if unfortunate, but not unreasonable, choices of the renormalization and factorizations scales are made in a computation based on leading order matrix elements. Note that the probability that an unfortunate scale choice is made increases for a larger number of jets since the production cross-section at LO becomes a steeper function of the renormalization and factorization scales. The only way to cure this problem is by computing NLO QCD corrections. For processes like $pp \rightarrow W + 4$ jets or $pp \rightarrow t\bar{t} + 2j$ this will be complicated no matter what method is used, but we believe that generalized unitarity will be up to the task.

Acknowledgments

We are grateful to W. Giele, Z. Kunszt and G. Salam for useful discussions. The research of K.M. is supported by the startup package provided by Johns Hopkins University. G.Z. is supported by the British Science and Technology Facilities Council. Fermilab is operated by Fermi Research Alliance, LLC under Contract No. DEAC02-07CH11359 with the United States Department of Energy.

References

- [1] Z. Bern *et al.* [NLO Multileg Working Group], arXiv:0803.0494 [hep-ph].
- [2] T. Aaltonen *et al.* [CDF Collaboration], Phys. Rev. D **77**, 011108 (2008) [arXiv:0711.4044 [hep-ex]].
- [3] T. Aaltonen *et al.* [CDF - Run II Collaboration], Phys. Rev. Lett. **100**, 102001 (2008) [arXiv:0711.3717 [hep-ex]].
- [4] J. Campbell and R. K. Ellis, Phys. Rev. D **65**, 113007 (2002) [arXiv:hep-ph/0202176].
- [5] G. Passarino and M. J. G. Veltman, Nucl. Phys. B **160**, 151 (1979).
- [6] A. I. Davydychev, Phys. Lett. B **263** (1991) 107.
- [7] G. Duplancic and B. Nizic, Eur. Phys. J. C **35** (2004) 105 [arXiv:hep-ph/0303184].
- [8] W. T. Giele and E. W. N. Glover, JHEP **0404** (2004) 029 [arXiv:hep-ph/0402152].
- [9] R. K. Ellis, W. T. Giele and G. Zanderighi, Phys. Rev. D **73** (2006) 014027 [arXiv:hep-ph/0508308].
- [10] A. Denner and S. Dittmaier, Nucl. Phys. B **734**, 62 (2006) [arXiv:hep-ph/0509141].
- [11] A. van Hameren, J. Vollinga and S. Weinzierl, Eur. Phys. J. C **41** (2005) 361 [arXiv:hep-ph/0502165].
- [12] T. Binoth, J. P. Guillet, G. Heinrich, E. Pilon and T. Reiter, arXiv:0810.0992 [hep-ph].
- [13] A. Denner, S. Dittmaier, M. Roth and L. H. Wieders, Phys. Lett. B **612**, 223 (2005) [arXiv:hep-ph/0502063].
- [14] R. K. Ellis, W. T. Giele and G. Zanderighi, JHEP **0605** (2006) 027 [arXiv:hep-ph/0602185].
- [15] A. Bredenstein, A. Denner, S. Dittmaier and S. Pozzorini, JHEP **0808** (2008) 108 [arXiv:0807.1248 [hep-ph]].
- [16] K. Arnold *et al.*, arXiv:0811.4559 [hep-ph].

- [17] D. E. Soper, Phys. Rev. Lett. **81**, 2638 (1998) [arXiv:hep-ph/9804454].
- [18] D. E. Soper, Phys. Rev. D **62**, 014009 (2000) [arXiv:hep-ph/9910292].
- [19] D. E. Soper, Phys. Rev. D **64**, 034018 (2001) [arXiv:hep-ph/0103262].
- [20] Z. Nagy and D. E. Soper, Phys. Rev. D **74**, 093006 (2006) [arXiv:hep-ph/0610028].
- [21] A. Lazopoulos, K. Melnikov and F. Petriello, Phys. Rev. D **76**, 014001 (2007) [arXiv:hep-ph/0703273].
- [22] A. Lazopoulos, K. Melnikov and F. J. Petriello, Phys. Rev. D **77**, 034021 (2008) [arXiv:0709.4044 [hep-ph]].
- [23] A. Lazopoulos, T. McElmurry, K. Melnikov and F. Petriello, Phys. Lett. B **666**, 62 (2008) [arXiv:0804.2220 [hep-ph]].
- [24] Z. Bern, L. J. Dixon, D. C. Dunbar and D. A. Kosower, Nucl. Phys. B **425**, 217 (1994) [arXiv:hep-ph/9403226].
- [25] Z. Bern, L. J. Dixon and D. A. Kosower, Nucl. Phys. B **513**, 3 (1998) [arXiv:hep-ph/9708239].
- [26] R. Britto, F. Cachazo and B. Feng, Nucl. Phys. B **725**, 275 (2005) [arXiv:hep-th/0412103].
- [27] R. Britto, F. Cachazo and B. Feng, Phys. Lett. B **611** (2005) 167 [arXiv:hep-th/0411107].
- [28] G. Ossola, C. G. Papadopoulos and R. Pittau, Nucl. Phys. B **763**, 147 (2007) [arXiv:hep-ph/0609007].
- [29] R. K. Ellis, W. T. Giele and Z. Kunszt, JHEP **0803**, 003 (2008) [arXiv:0708.2398 [hep-ph]].
- [30] R. K. Ellis, W. T. Giele and Z. Kunszt, PoS **RADCOR2007**, 020 (2007) [arXiv:0802.4227 [hep-ph]].
- [31] C. F. Berger *et al.*, Phys. Rev. D **78** (2008) 036003 [arXiv:0803.4180 [hep-ph]].
- [32] W. T. Giele, Z. Kunszt and K. Melnikov, JHEP **0804**, 049 (2008) [arXiv:0801.2237 [hep-ph]].
- [33] see R. K. Ellis and G. Zanderighi, JHEP **0802**, 002 (2008) [arXiv:0712.1851 [hep-ph]] and references therein.
- [34] W. T. Giele and G. Zanderighi, JHEP **0806**, 038 (2008) [arXiv:0805.2152 [hep-ph]].
- [35] R. K. Ellis, W. T. Giele, Z. Kunszt and K. Melnikov, arXiv:0806.3467 [hep-ph].

- [36] R. K. Ellis, W. T. Giele, Z. Kunszt, K. Melnikov and G. Zanderighi, JHEP **0801**, 012 (2009) [arXiv:0810.2762 [hep-ph]].
- [37] T. Binoth, G. Ossola, G.G. Papadopoulos, R. Pittau, JHEP **0806** (2008) 082.
- [38] C. F. Berger *et al.*, arXiv:0808.0941 [hep-ph].
- [39] R. K. Ellis, D. A. Ross and A. E. Terrano, Nucl. Phys. B **178**, 421 (1981).
- [40] S. Catani and M. H. Seymour, Nucl. Phys. B **485**, 291 (1997) [Erratum-ibid. B **510**, 503 (1998)] [arXiv:hep-ph/9605323].
- [41] Z. Nagy, Phys. Rev. D **68**, 094002 (2003) [arXiv:hep-ph/0307268].
- [42] G. P. Lepage, J. Comput. Phys. **27**, 192 (1978).
- [43] M. H. Seymour and C. Tevlin, arXiv:0803.2231 [hep-ph].
- [44] V. Del Duca, L. J. Dixon and F. Maltoni, Nucl. Phys. B **571**, 51 (2000) [arXiv:hep-ph/9910563].
- [45] Z. Bern, L. J. Dixon and D. A. Kosower, Nucl. Phys. B **437**, 259 (1995) [arXiv:hep-ph/9409393].
- [46] J. Pumplin, D. R. Stump, J. Huston, H. L. Lai, P. M. Nadolsky and W. K. Tung, JHEP **0207**, 012 (2002) [arXiv:hep-ph/0201195].
- [47] J. Campbell, R. K. Ellis and D. L. Rainwater, Phys. Rev. D **68** (2003) 094021 [arXiv:hep-ph/0308195].